Perilla seed oil high internal phase emulsion improve the gel properties of myofibrillar protein

Beibei Li [a,b], Yang Wang [a,b], Shuyu Wang [a,b], Sengao Chen [a,b], Chaoyue Yang [a,b], Linggao Liu [a,b], Shenghui Bi [a,b], Ying Zhou [a,b,*], Qiujin Zhu [a,b,c,*]

[a] School of Liquor and Food Engineering, Guizhou University, Guiyang 550025, China
[b] Key Laboratory of Agricultural and Animal Products Store and Processing of Guizhou Province, Guiyang 550025, China
[c] Key Laboratory Mountain Plateau Animals Genetics and Breeding, Ministry of Education, Guiyang 550025, China

A R T I C L E I N F O

A B S T R A C T

The effects of perilla seed oil high internal phase emulsions stabilized by pea protein (PP-PSO HIPEs) on the gel properties and conformation of myofibrillar protein (MP) gels were investigated. The results showed that the PP-PSO HIPEs with 4.0 % (w/v) PP formed stable HIPEs with low droplet size and good viscoelasticity. The addition of PP-PSO HIPEs (5.0 % − 15.0 %) could significantly improve the MP gel properties ($P < 0.05$), while the addition of 10.0 % PP-PSO HIPEs showed the highest gel strength and water holding capacity. Otherwise, the MP gels with 10.0 % PP-PSO HIPEs showed higher proportions of immobile water (PT_{22}) and lower proportion of free water (PT_{23}), and the Raman spectra suggested that the content of α-helix decreased, while the content of β-sheet increased ($P < 0.05$), thus facilitating the formation of better gel properties. Therefore, the addition of PP-PSO HIPEs is a potential alternative for developing fat-reduced meat products.

1. Introduction

In recent years, the risk of obesity, atherosclerosis, coronary heart disease and other chronic diseases had been increased which could be attributed to the high content of fat and unhealthy fatty acids in animal fat (Badar, Liu, Chen, Xia, & Kong, 2021). WHO (2022) emphasized that in order to ensure a healthy diet, total fat intake must be controlled to less than 30 %, and saturated fat intake must be controlled to less than 10 % of total energy. Researchers had used vegetable oils such as rapeseed oil, olive oil, and corn oil to replace animal fat, but the substitution effect could not achieve desired state. Even though the content of saturated fatty acids in the products had been reduced, compared with full-fat products, the low-fat meat products had low overall acceptance, with decreased water holding capacity (WHC) and deteriorated texture (Bibat, Ang, & Eun, 2022; Shao, Bi, Dai, & Li, 2020). Some researchers had also used plant proteins and polysaccharides as fat substitutes, but they could not simulate the product quality brought by animal fat (Ruiz-Capillas, Triki, Herrero, Rodriguez-Salas, & Jimenez-Colmenero, 2012). Therefore, how to reduce the content of animal fat on the premise of ensuring the quality of gel-type meat products was still a major problem in the meat industry.

Pre-emulsification of certain vegetable oils with non-meat proteins was a processing method proposed in recent years to replace animal fat in gel-type meat products. Compared with the traditional method of directly mixing all materials, pre-emulsified vegetable oil could increase the stability of vegetable oil, which could be applied in reduced fat meat products, particularly those rich in polyunsaturated fatty acid (PUFA) (Buamard & Benjakul, 2019). During the pre-emulsification process, the added protein could be directly adsorbed on the surface of the oil droplet to form a protein film and reduced its interfacial tension, so the wrapped small fat balls will be relatively stable when added to the minced meat. During meat processing, a large amount of salt soluble protein was needed to emulsify fat globules by traditional methods. However, in the process of pre-emulsification, the added protein was more targeted on the oil, greatly reducing the content of myosin involved in the emulsification process, and promoting more myosin to participate in the gel process, which could help to form the gel network structure and avoid the problem of poor elasticity and loose texture of surimi sausage (Liu, Ji, Zhang, Xue, & Xue, 2019). Emulsions with an oil volume fraction of more than 74 % could be considered as high internal phase emulsions (HIPEs). Due to its large oil phase volume fraction, HIPEs system was a solid like gel, also known as gel emulsion, HIPEs had a high strength

---

interface layer and a tight and ordered structure, so its structure had good stability (Zhou, Drusch, & Hogan, 2023). Fontes-Candia et al. (2023) reported that the emulsion gel could effectively reduce the fat content in meat products, without lowering the sensory properties, as well as improving the WHC and texture.

Perilla seed oil (PSO) was a vegetable oil with over than 90 % of unsaturated fatty acids, which rich in n-3 series unsaturated fatty acids, especially α-linolenic acid (Hu, Xie, Zhang, Li, & Qi, 2020). Ran, Chen, Li, He, and Zeng (2020) had shown that PSO could provide essential fatty acids, reduce cholesterol, regulate blood pressure, prevent cancer and anti-aging et al. Pea protein (PP) is a plant protein with hypo-allergenicity, complete essential amino acid spectrum and high content of lysine and tryptophan. In addition, PP is a good source of bioactive peptides, which is beneficial to human health. Similar to soy protein, PP also exhibited some functional properties, such as strong emulsification ability, and therefore had great market potential (Kornet, Yang, Venema, van der Linden, & Sagis, 2022). Therefore, the HIPEs based on PSO and PP was a promising alternative for fat-reduced meat products, but it remained minimally studied.

The emulsification and the gelation processes of myofibrillar proteins (MP) were the most important processing characteristics in the processing of gel-type meat products. The gel properties of processed meat products mainly depend on the functional properties of MP. MP molecules or other non-protein components will interact with each other through chemical or physical ways to form gel network structure. The texture, WHC, and stability of meat products were determined by their gel structure (Shi, Zhou, Wang, Zou, Wang, & Xu, 2021). Wang et al. (2023) found that adding Tenebrio molitor protein emulsions improved the structural stability of MP gel. However, the components in the emulsion and the role of MP were complicated, the effects and mechanism still need further study. The addition of pea protein-perilla seed oil HIPEs (PP-PSO HIPEs) to MP gel were rarely studied, so the mechanism of its effect on the gel properties of MP was not clear. This study was to provide an in-depth understanding to provide a theoretical basis for the development of low-fat meat products.

Based on this, in this study, PP-PSO HIPEs was prepared by PP and PSO. And the the droplet size distribution, ζ-potential, microstructure and centrifugal stability of PP-PSO HIPEs were analyzed, the MP gel properties, water distribution and protein secondary structure of MP gel were investigated by adding the PP-PSO HIPEs directly to the MP gel. This study provided a understanding on how the PP-PSO HIPEs influenced the MP gels and a theoretical basis for developing healthy, low fat meat products in the future.

2. Materials and methods

2.1. Materials

Pork tenderloin was purchased from WalMart supermarket (Guiyang, China), PSO was obtained from Hebei Jiafeng Vegetable Oil Co., Ltd. (Hebei, China) and PP was obtained from Chengdu Mairen Biotechnology Co., Ltd (Sichuan, China). All other chemicals used in these experiments were analytical grade.

2.2. Preparation of PP-PSO HIPEs

The PP was added into distilled water to reach a certain concentration of 1.0 %, 2.0 %, 3.0 %, 4.0 %, and 5.0 % (w/v), stir at 25 °C for 2 h until fully dissolved. To ensure adequate hydration of the PP solution, then keep it overnight at 4 °C. PSO ($\varphi = 0.75$) was added to the PP solution, and PP-PSO HIPEs were prepared by homogenizing at 10,000 r/min for 1 min with XHF-DY high-speed disperser (Ningbo Scientz Biotechnology Co., Ltd., Zhejiang, China).

2.3. Characterization of the PP-PSO HIPEs

2.3.1. Measurement of emulsion droplet ζ-potential and size

The droplet size distribution of PP-PSO HIPEs was measured using the laser diffraction particle size analyzer (LS 13320, Beckman, California, USA). Before measurement, all the samples were diluted 50-fold with distilled water. The ζ-potential values of the droplets in the PP-PSO HIPEs were measured using a wide dynamic range (high concentration) potential and nanoparticle size production analyzer (DelsaNanoC, Beckman Coulter, Inc) at 25 °C. The refractive index (RI) of PSO and water was set at 1.467 and 1.330, respectively, while the absorption parameter was 0.001.

2.3.2. Optical microscopy

Before testing, it was necessary to dilute the samples six times with pure water due to the gel like nature of PP-PSO HIPEs. The 10 μL of sample was aspirated and placed onto the slide, and the micrographs of the emulsion were observed with an optical microscope (DMEX20, Ningbo Shunyu Instrument Co., Ltd., Zhejiang, China) to evaluate the size and aggregation state of the PP-PSO HIPEs droplets.

2.3.3. Rheological measurements

According to Wang et al. (2023), a rotational rheometer (Mars 60, Haake, Germany) was used with a plate-to-plate geometry (diameter 20 mm). To obtain a stable shear viscosity, the shear rate was gradually increased from 0.1 s^{-1} to 100 s^{-1} while the apparent viscosity at each stage was recorded. Under constant strain conditions of 1 %, the measurement of storage modulus (G') and loss modulus (G'') were conducted with a frequency sweep ranging from 0.1 to 10 rad/s. The entire experiment was conducted in a constant temperature environment.

2.3.4. Centrifugal stability

The 15 g PP-PSO HIPEs were placed in centrifuge tube and centrifuged with a centrifuge (TGL-20 M Hunan Michael Experimental Instrument Co., LTD.) at 10,000 g for 15 min at 25 °C. Centrifugal stability of HIPEs is calculated by the following formula:

$$\text{Centrifugal stability (\%)} = W_0\text{-}W_1/W_0 \times 100$$

W_0 represented the total weight of the PP-PSO HIPEs before centrifugation, while W_1 represented the weight of the combined oil and water that separated after centrifugation.

2.3.5. Confocal laser scanning microscope (CLSM) observation

A laser confocal microscope (LSM900, German card zeiss, Germany) was used to observe the HIPEs. The protein and oil phases were stained using 0.1 % Nile Blue A and 0.01 % Nile Red, respectively. Transfer the dyed emulsions onto a microscope slide, and then cover it with a clean cover slide. In the experiment, a 20 × lens was utilized, and excitation wavelengths of 488 nm and 633 nm were selected.

2.4. Preparation of myofibrillar protein (MP)

The MP was prepared using the methods outlined by Zhu, Wang, Zong, Zhang, Zhao, and Ma (2024) with minor modifications. Fresh pork tenderloin was removed, connective tissue, fat, and other impurities were removed, and minced. The mince was homogenized twice with an ice bath by a high-speed disperser with phosphate buffer (0.1 mol/L KCl, 1 mmol/L MgCl$_2$, 7 mmol/L KH$_2$PO$_4$, 18 mmol/L K$_2$HPO$_4$, 1 mmol/L EGTA, pH 7.0) at 3000 r/min for 30 s. Subsequently, the homogenate was subjected to centrifugation at 2000 g for 10 min at 4 °C using a high-speed refrigerated centrifuge and the resulting precipitate was collected. After repeating the above process three times, the obtained precipitate was thoroughly mixed with a phosphate buffer (0.1 mol/L NaCl, pH 6.0) for 30 s and then subjected to another centrifugation at 2000 g for 10 min. This process was carried out three times at 4 °C, resulting in the

identification of the precipitate as MP.

2.5. Preparation of MP gels with PP-PSO HIPEs

Based on the previous results, a PP-PSO HIPEs with PP concentration of 4.0 % (w/v) was for a follow-up study. The MP was dissolved in a phosphate buffer (0.6 mol/L NaCl, 50 mmol/L Na_2HPO_4, pH 6.5). The concentration of MP was determined using the BCA Protein Assay Kit (Beijing Solarbio Science & Technology Co., Ltd., Beijing, China) according to the instructions, and adjusted to 35 mg/mL. After that, the PP-PSO HIPEs were added to prepared MP solutions, with the content of PP-PSO HIPEs being 0.0 %, 5.0 %, 10.0 %, 15.0 %, and 20.0 % (w/w), respectively. The moisture content was adjusted using distilled water to ensure that all sample groups had the same moisture content. A high-speed disperser was applied to homogenize the mixtures, which were transferred to a sealed glass bottle (25 × 40 mm, diameter × height) and heated up linearly from room temperature to 80 °C, hold at 80 °C for 30 min to form a gel, then quickly remove from the water bath and quickly put into ice bath to cool for 10 min, then stand overnight at 4 °C for subsequent measurements.

2.6. Determination of MP gels quality

2.6.1. Gel strength

The gel strength of MP gels was performed by using a TA. TOUCH texture analyzer (Bao Sheng Technology Co., Ltd., Shanghai, China). Prior to measurement, the gels needed to be equilibrated at room temperature for 2 h. A gel probe (diameter 12.7 mm) used in the analysis, before test speed: 1.50 mm /s, test speed: 0.5 mm/s, after test speed: 0.50 mm /s, trigger force: 5.0 g, displacement: 8 mm. The force (breaking force) of the piercing gel and the distance (deformation) of the plunger piercing gel were recorded and the experiment was repeated 5 times.

2.6.2. Whiteness

The colorimeter (Shenzhen TILO Tech. Co.,Ltd., Guangdong, China) was used for gels whiteness analysis. Before using the colorimeter, it was initially calibrated using a standard whiteboard. L* (brightness), a* (red), b* (yellow) was measured and recorded, all samples were repeatedly measured six times, the results were averaged, and then the whiteness value was calculated according to the following formula:

$$Whiteness = 100 - \sqrt{(100 - L*)^2 + a*^2 + b*^2}$$

2.6.3. Water-holding capacity (WHC)

Weighed about 7 g of gel, putted it in a centrifuge tube, centrifuged at 8000 g for 15 min at 4 °C, then absorbed the water on the surface of MP gels with absorbent paper, and weighed. The experiment was replicated 4 times. WHC was calculated according to the following formula:

WHC (%) = (W_2 / W_1) × 100.

The W_1 represented the weight of MP gel before centrifugation, and W_2 represented the weight of MP gel after centrifugation.

2.6.4. Low-field nuclear magnetic resonance (LF-NMR)

The moisture distributions of the MP gels were measured using an LF-NMR analyzer (NMI 20–040 V-I, Neumag Analytical Instruments, Suzhou, China) with a proton frequency of 21 MHz. The specific determination methods are as follows: The sample was cut into a cylinder of the same mass (diameter 15 mm, height 40 mm) and placed in a glass vial, the glass vial was placed in an NMR tube (diameter 25 mm), and the nuclear magnetic tube was placed in the LF-NMR sample chamber for 1 min. The Carr-Purcell-Meiboom-Gill (CPMG) sequence was used to obtain T_2 at 32 °C. The test conditions are as follows: TW (ms) = 6000, NS = 8, TE (ms) = 0.250, NECH = 18000.

2.6.5. Raman spectra measurements

The Raman spectra was based on the method of Kang, Wang, Xu, Zhu, Li, and Zhou (2014), with a minor modification, using a micro-confocal laser Raman spectrometer (HR Evolution, HORIBA Jobin Yvon, France) with a 532 nm laser source. The MP gels were freeze-dried for 48 h and then determined. The protein samples were laid on a slide, the laser was first focused on the sample using a 50 × long focal length lens, and then the Raman signal of 400–2000 cm^{-1} was collected. The determination parameters were: resolution was 2 cm^{-1}, exposure time was 60 s, and each sample was scanned 5 times. The resulting spectra were smoothed using Labspec6 analysis software, and the multipoint baseline was positive to remove the fluorescent background. The resulting spectra were smoothed using Labspec6 analysis software, and the multipoint baseline was positive to remove the fluorescent background.

2.6.6. Reactive sulfhydryl content

According to the method previously described by Shen, Elmore, Zhao, and Sun (2020) with a little modifications, 8 g MP gels was weighed and dissolved in 22 mL 20 mM Tris-HCl buffer (10 mmol/L EDTA, 0.6 mol/L KCl pH 7.0) and homogenized with a homogenizer at 10,000 rpm for 30 s. Then the homogenate was centrifuged in a high-speed refrigerated centrifuge at 10,000 g for 10 min at 4 °C, the protein concentration in the supernatant was determined using the BCA Protein Assay Kit and adjusted to 1 mg/mL. 5.5 mL protein solution was mixed with 0.1 mL DTNB (10 mmol/L) and placed at 4 °C for 1 h to determine the absorbance of the solution at 412 nm. The content of reactive sulfhydryl was calculated. The molar absorption coefficient of sulfhydryl group is 13,600 $M^{-1} \cdot cm^{-1}$.

2.6.7. Surface hydrophobicity

The MP solution was diluted to 5 mg/mL with phosphate buffer (pH 6.5), and 200 μL of bromophenol blue (BPB) solution (1 mg/mL, dissolved in deionized water) was added to 1 mL of MP solution and mixed. The corresponding buffer was used as a control group. The sample and control groups were mixed at room temperature for 10 min and centrifuged (2000 g, 15 min). The centrifuged supernatant was diluted 10-fold and the absorbance value (A) was determined at 595 nm, and the control group was BPB phosphate buffer (A_0). Surface hydrophobicity was calculated by the following formula:

BPB bound (μg) = 200 μg × (A-A_0) /A_0

2.7. Statistical analysis

The experimental results were expressed as the mean ± standard deviation of at least three independent samples. Significant differences between different groups ($P < 0.05$) were determined by Duncan's multiple range test and ANOVA by IBM SPSS 27 (SPSS, Inc., Chicago, Illinois, USA). All figures were drawn using Origin 2022.

3. Results and discussion

3.1. Characterization of the PP-PSO HIPEs

3.1.1. Droplet size distribution, ζ -potential and microstructure of PP-PSO HIPEs

The droplet size distribution can reflect the degree of stability of the emulsion to a certain extent, the stability of emulsion generally improve with the decrease of particle size. Fig. 1(a) depicted the effect of PP concentration on the droplet size distribution in PP-PSO HIPEs. The droplet size of PP-PSO HIPEs stabilized by PP decreased significantly from 65.23 to 23.39 μm while the PP concentration increased from 1.0 % to 4.0 % (w/v). This trend was consistent with the optical microscopic
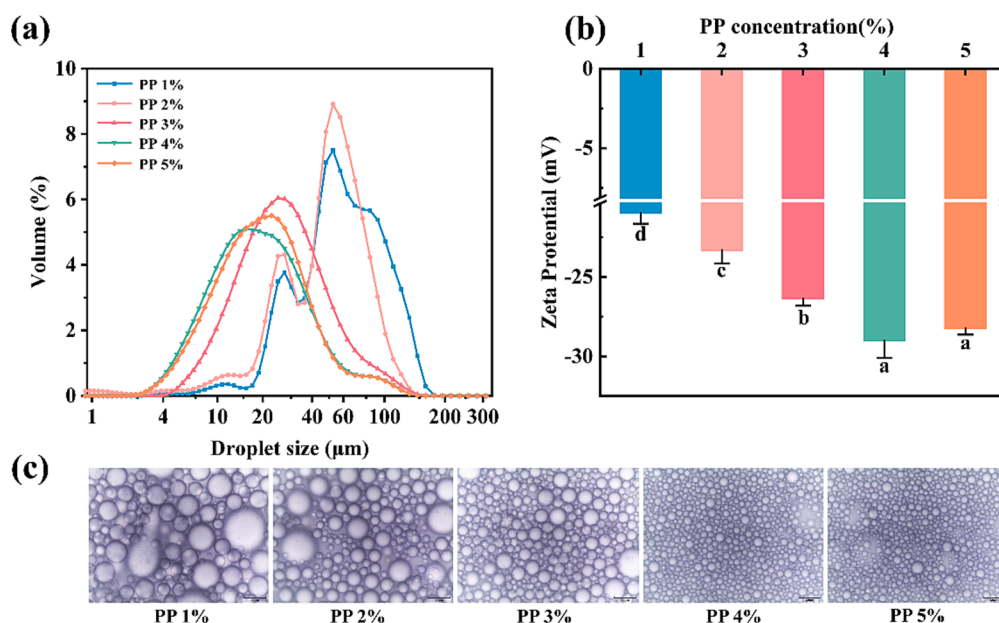
Fig.1. Effect of PP concentration on the performance of PP-PSO HIPEs. (a) droplet size distribution, (b) ζ-potential (*a-d on the histograms indicates that the different letters are significantly different ($P < 0.05$).), (c) optical microscope image (five times diluted with deionized water, scale: 60 μm).

images of the PP-PSO HIPEs (Fig. 1(c)). The sample with 1.0 % PP exhibited two dominant peaks (30 μm and 59 μm, respectively), and the second peak had a wider distribution range (35–200 μm), suggesting a larger and non-uniform droplet distribution of PP-PSO HIPEs with 1.0 % PP, which was consistent with its optical microscopic images (Fig. 1(c)). The PP concentration increased to 3.0 % resulted in a leftward shift of the droplet distribution peak, which exhibited a single peak at 26.04 μm. This indicated smaller and more uniform droplet sizes, suggesting a higher emulsifying capacity. When the PP concentration was added to 4.0 %, the droplet distribution peak shifted more significantly to the left (18.14 μm). Furthermore, no significant difference in droplet size distribution was observed between the 4.0 % and 5.0 % protein concentrations. The fact that PP and PSO formed a barrier during emulsification, hindering the aggregation of oil droplets and reducing the interfacial tension, could explain this phenomenon. Thus, with the increase of PP concentration, the formed emulsion droplets became smaller. When there was already enough PP to stabilize the oil–water interface, the increase of the protein particle concentration could not further decrease the droplet size of the emulsion (Lin et al., 2021).

The proteins in the emulsion adsorbed to the surface of the oil droplets to provide an electrical charge. The ζ-potential of PP-PSO HIPEs was shown in Fig. 1(b). The PP-PSO HIPEs stabilized by 1.0 % PP exhibited the lowest absolute ζ-potential value (-20.96 mV). A significant increase ($P < 0.05$) in absolute ζ-potential values was observed in the PP-PSO HIPEs as the PP concentration was increased to 4.0 % (-29.00 mV), suggesting greater electronegativity and stronger interparticle electrostatic repulsion. The growth was likely due to an increase in protein concentration in the emulsion system, leading to an increase in the adsorption of proteins at the oil–water interface, and an enhancement in the surface charged on the droplets. Thus, the increase in the electrostatic repulsion among the droplets induced a suppression of droplet aggregation, ultimately improving the stability of the PP-PSO HIPEs (Hu et al., 2021).

3.1.2. Centrifugal stability

As shown in Fig. 2, the PP-PSO HIPEs stabilized by lower PP concentrations (1.0 % − 3.0 %) displayed varying levels of oil leakage suggesting a low centrifugal stability. This meant that the concentration of PP was too low to encapsulate all the oil droplets. As the PP concentration increased, the centrifugal stability index of the emulsion
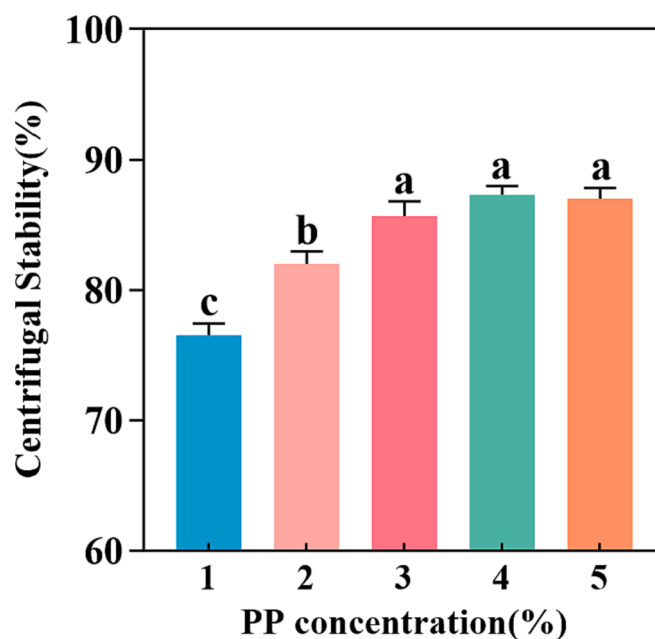

Fig. 2. Effect of PP concentration on the centrifugal stability of PP-PSO HIPEs. *a-c on the histograms indicates that the different letters are significantly different ($P < 0.05$).

exhibited an upward trend until it reached at 3.0 % PP concentration. With further increase of PP concentration to 4.0 % − 5.0 %, there is no longer any oil leakage occurring and larger volume of emulsion layer formed. This was attributed to the formation of a denser barrier at the oil–water interface during the emulsification process. Besides, there were traces of water released after centrifugation, which could be relate to that the PP had high hydrophobicity and poor WHC (Li, Liu, Xu, & Zhang, 2022). With the PP concentration increased, less water leaked after centrifugation, which showed that the gel-like network of PP-PSO HIPEs with low concentration of PP were more fragile than that of PP-PSO HIPEs with high concentration of PP, thus leading to lower capillary forces and centrifugal stability.

3.1.3. Rheological measurements

The rheological properties of HIPEs were closely linked to their microstructure and storage stability. As depicted in Fig. 3(a), the apparent viscosity of all PP-PSO HIPEs decreased gradually and tended to zero with the shear rate increased. This demonstrated the shear thinning behavior of pseudoplastic non-Newtonian fluids. This might be attributed to the rupture of the protein film on the surface of the oil droplets with the shear rate increased, leading aggregation of the oil droplets and decrease of the apparent viscosity (Wan et al., 2017).

As the concentration of PP increased, the apparent viscosity increased significantly, with the highest viscosity obtained at 4.0 % PP. The most likely explanation was that when the PP concentration was low, the PP in the system was not enough to stabilize the PP-PSO HIPEs. However, as the PP concentration increased gradually, the more amount of protein will be adsorbed at the interface of the interfacial film. At this time, a viscoelastic spatial network structure with a certain strength was formed, so it had superior viscoelasticity (Wang, Wang, Dai, Yu, & Cheng, 2023).

As shown in Fig. 3(b), the G' values of all PP-PSO HIPEs were higher than that of the G'' values, indicating that these PP-PSO HIPEs might exhibit elastic properties (Niknam, Ghanbarzadeh, Ayaseh, & Rezagholi, 2018). The increase of PP concentration resulted in a gradual increase in both G' and G'', indicating that the PP-PSO HIPEs system with higher PP concentration exhibited improved plasticity and enhanced rigidity. This might be due to the fact that as protein concentration increased, the more particles will be participated in the construction of the emulsified gel system. Moreover, the tight packing of the small, dense droplets leads to enhanced physical cross-linking between PP at the interface, accelerating the rearrangement of the gel network. Consequently, this strengthens the network structure within the PP-PSO HIPEs (Zhang, Cheng, Luo, Hemar, & Yang, 2021). Therefore, the enhancement of the network structure will cause the gradual improvement of elasticity as well as gel properties, thus the increase in the energy storage modulus.

3.1.4. CLSM

The microstructure of PP-PSO HIPEs stabilized by different concentrations of PP were depicted in Fig. 4, showing the aqueous phase, the oil phase, and the combined oil–water phase (from left to right). The green oil phase was located in the interior of the droplet with PP (marked in red) formed a clear boundary on the droplet's surface to prevent coalescence as a barrier. With the increase of PP concentrations, the volume
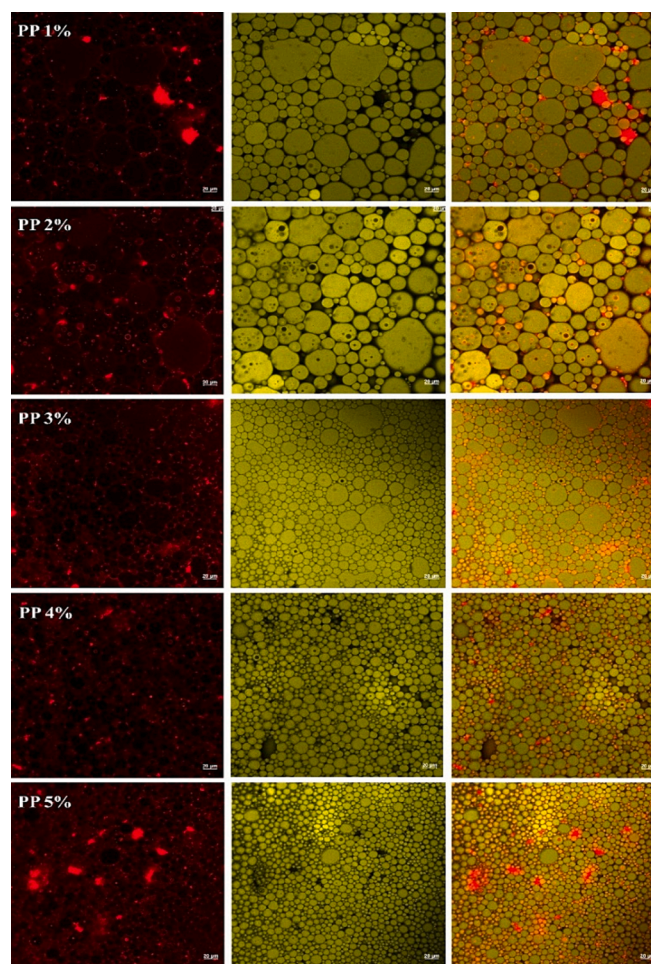

Fig.4. Confocal laser scanning microscopy (CLSM) images of the PP-PSO HIPEs stabilized by different concentrations of PP. The aqueous phase was labeled with Nile blue (in red), and the oil phase was labeled with Nile red (in green). Scale 20 μm. (For interpretation of the references to color in this figure legend, the reader is referred to the web version of this article.)
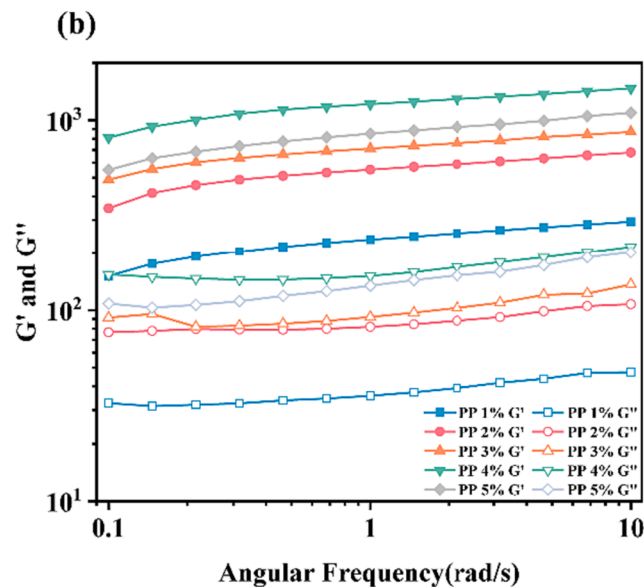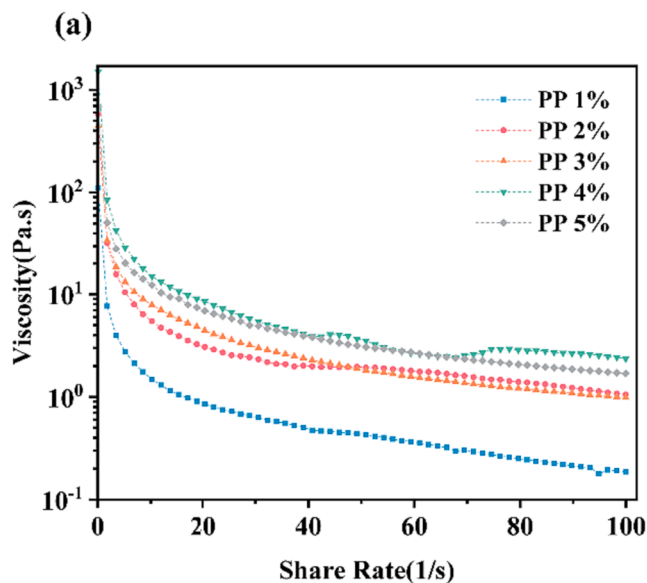

Fig.3. Rheological properties of the PP-PSO HIPEs stabilized by different concentrations of PP. (a) Apparent viscosity of the PP-PSO HIPEs with shear rate from 0.1 to 100 1/s; (b) Frequency sweeps curves at fixed stain (1 %) with frequency ranging from 0.1 to 10 rad/s.

of the emulsion droplets becoming more uniform, which was consistent with the droplet size distribution (Fig. 1(a)) and the optical microscopy (Fig. 1(c)).

3.2. Characterization of MP gel quality

3.2.1. Gel strength

Based on the previous results, a PP-PSO HIPEs with PP concentration of 4.0 % (w/v) was for a follow-up study. The gel strength of MP gel was the mainly property that responsible for the quality of emulsified meat products. Fig. 5(a) illustrated that the addition of PP-PSO HIPEs significantly improved the gel strength ($P < 0.05$). Compared with the group that without PP-PSO HIPEs, the addition of 5.0 %−10.0 % PP-PSO HIPEs to MP induced a significant enhancement in the MP gel strength ($P < 0.05$). The observed enhancement in gel strength might be attributed to the increase of hydrophobic interaction and the intermolecular interaction between MP and PP in PP-PSO HIPEs (Buamard & Benjakul, 2019). The PP-PSO HIPEs were uniformly dispersed within MP matrix, leading to the formation of a gel network during heating. The small droplets in the PP-PSO HIPEs enhanced the cross-linking between protein molecules in MP gels and thereby increased the gel strength (Wang et al., 2023). Lee, Jang, Kang, and Chin (2017) have shown that incorporating nonmeat proteins into reduced-salt pork MP can significantly enhance the texture properties of gels.

Furthermore, incorporating PP-PSO HIPEs with favorable viscoelasticity into the gel network formed by MP led to an enhancement in the performance of the MP gel, the degree of gel cohesion was increased, making the structure compact, and thus the gel strength rised (Zhuang et al., 2016). However, as the addition amount of PP-PSO HIPEs increased until reaching 15.0 %−20.0 %, the gel strength of MP

significantly decreased ($P < 0.05$), which could likely be attributed to the limited ability of MP to encapsulate the PP-PSO HIPEs (Lin et al., 2019).

3.2.2. Whiteness

The whiteness of the gel could serve as an indicator of both the color and quality attributes of MP gels. The change in gel color could be strongly attributed to the protein oxidative denaturation the WHC of the gel, and the light scattering effect of oil droplets (Shi, Wang, Chang, Wang, Yang, & Cui, 2014). The impact of PP-PSO HIPEs on the whiteness of MP gels was shown in Fig. 5(c). The whiteness of MP gels with added PP-PSO HIPEs was significantly higher than that of MP gels without PP-PSO HIPEs, and the MP gels whiteness increased significantly with an increase in the amount of PP-PSO HIPEs added ($P < 0.05$). This observed phenomenon might be associated with the light scattering effect induced by the presence of oil droplets in PP-PSO HIPEs. Gani & Benjakul (2018) also found similar results that the nano-emulsions contained emulsified oil droplets with smaller particle sizes, further enhancing the light scattering effect and improving the MP gels whiteness.

3.2.3. WHC

WHC was not only utilized to evaluate the water holding capacity of MP gels, but also frequently employed to assess the quality of meat products. Higher WHC meant that MP gels, when heated and cooled, produced a more compact and uniform gel network that retained more water, fat, and other components. As can be seen in Fig. 5(b), the WHC of MP gels increased significantly ($P < 0.05$) from 75.76 % to 83.95 % with the increase addition of PP-PSO HIPEs from 0.0 % to 10.0 %. This result might be due to the void-filling effect of the oil droplets which leaded to
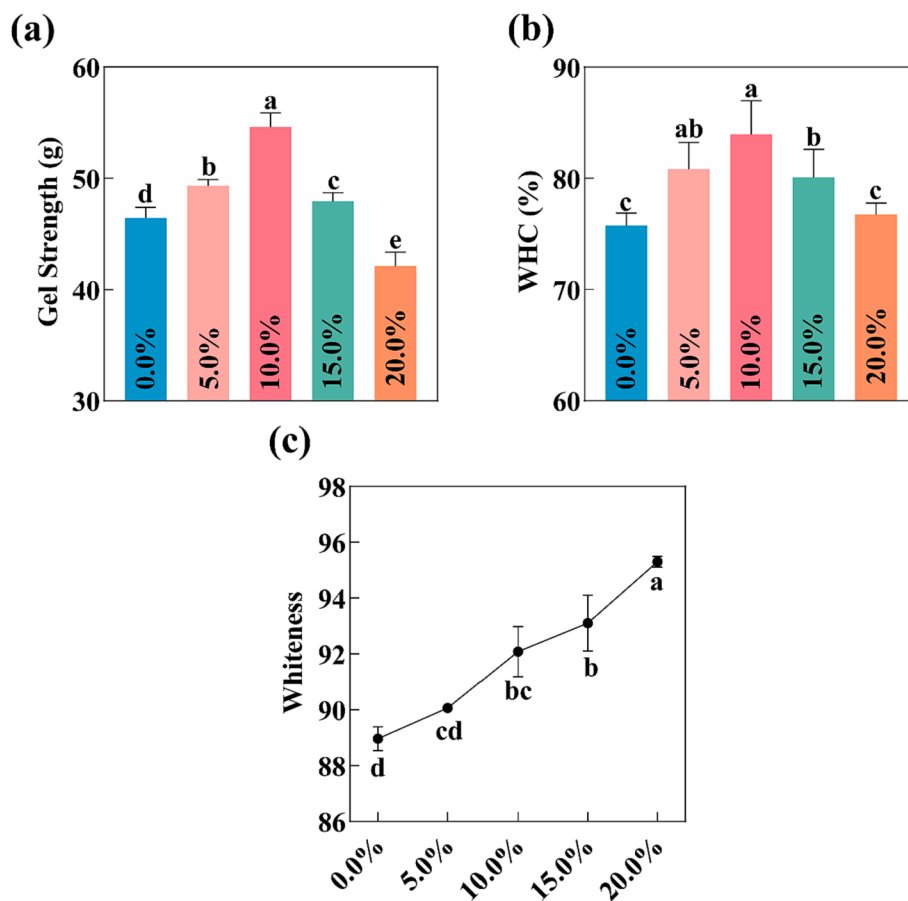

Fig.5. Effects of the addition (0.0% − 20%) of PP-PSO HIPEs on gel strength (a), WHC (b), and color (c) of MP gel. *a-d on the histograms indicates that the different letters are significantly different ($P < 0.05$).

a reduction in water fluidity (Wang et al., 2023a). The WHC of MP gels with 15.0 % − 20.0 % PP-PSO HIPEs gradually decreased, this phenomenon might be related to the fact the excess PP-PSO HIPEs aggregated in the gel network, disrupting the continuity of the gel network, affecting the dense structure of the gel, thus and reduced the WHC of MP gel. Therefore, the addition of PP-PSO HIPEs facilitated the formation of a uniformly distributed, compact, and highly organized gel network structure of MP, which effectively trapped water within its matrix and mitigated water migration.

3.2.4. Low-field nuclear magnetic resonance (LF-NMR)

As shown in Fig. 6(a), each sample exhibited four peaks on the relaxation time curves, corresponding to relaxation times of approximately 1–10 ms (T_{2b}), 10–100 ms (T_{21}), 100–1000 ms (T_{22}), and 1000–10000 ms (T_{23}), which correspond to the strongly bound water, weakly bound water, immobile water, and free water (Yang et al., 2020). The addition of 5.0 % − 10.0 % PP-PSO HIPEs resulted in a decrease in the T_{21}, T_{22}, and T_{23} of the MP gels, when compared with the control group, while the MP gels with 20.0 % PP-PSO HIPEs increased again.

The proportion of different states of water that distributed in the MP gels were depicted in Fig. 6(b), as determined by peak area. With the addition of PP-PSO HIPEs up to 15.0 %, the proportion of immobile water (PT_{22}) increased and the proportion of free water (PT_{23}) decreased, which confirms that the conversion of free water into immobile water in the MP gel. This finding was accordance with the results of WHC (Fig. 5(b)). The result might be due to the uniform distribution of small oil droplets within the MP gel in the PP-PSO HIPEs, which leaded to a tighter and more uniform gel network structure (Zhang, Xie, Liang, Jiang, Zhang, & Shi, 2023). However, the PT_{22} of the MP gels with 20.0 % PP-PSO HIPEs addition decreased and the PT_{23} increased, indicating that excess PP-PSO HIPEs could decrease the immobile water. The possible cause might lead to this phenomenon that the excess PP-PSO HIPEs aggregated in the gel network, which negatively affected the continuity of the gel network, compromised its dense structure, and ultimately resulted in a reduction of its WHC. Similar results were observed by Cen, Yu, Gao, Yang, Tang, and Feng (2022) who found that the addition of quinoa protein Pickering emulsions had the potential to enhance the proportion of immobile water and excessive amount of quinoa protein Pickering emulsions could lead to a reduction in the proportion of immobile water.

3.2.5. Secondary structure conformations

The effect of PP-PSO HIPEs on the secondary structure of MP was studied via Raman spectroscopy. The investigation of protein structure changes could be achieved by analyzing the variations in α-helix (1645–1658 cm^{-1}), β-sheet (1665–1680 cm^{-1}), β-turn (1680–1690 cm^{-1}) and random coil (1660–1665 cm^{-1}) (Cai, Nian, Cao, Zhang, & Li, 2020). According to Table 1, the α-helices content of MP gel decreased and the β-sheet content increased significantly with 10.0 % of PP-PSO HIPEs ($P < 0.05$), when compared with the control group. The β-sheet structure was more ordered than that of the natural spherical molecules, and the gel structure with higher β-sheet content was denser (Cando, Herranz, Javier Borderias, & Moreno, 2015). Chen and Han (2011) also reported that the gel strength and WHC of the gel increased, with the decrease of α-helix structure and the increase of β-sheet structure. The addition of PP-PSO HIPEs might promote the unfolding of α-helix, resulting in the exposure of more hydrophobic groups within the MP gel. As a result, the surface hydrophobicity (H_0) of MP also increased, thereby enhancing the hydrophobic interaction between MP molecules. According to Table 1, the H_0 of MP with 5.0 % − 15.0 % PP-PSO HIPEs was significantly higher ($P < 0.05$) than the MP gels without PP-PSO HIPEs. Wang, Zhang, Liu, Wang, Li, and Li (2024) studied the effect of Pickering emulsion with sodium starch octenyl succinate (SSOS) on hairtail MP gels, and the analysis of Raman spectra revealed that the Pickering emulsion played a pivotal role in facilitating the transformation of the secondary structure of MP, improved hydrophobic interactions. However, the content of α-helix structure increased in our study, when the addition amount of PP-PSO HIPEs reached 20.0 %, which may be due to the aggregation of excessive PP-PSO HIPEs that affected the unfolding of MP molecules.

3.2.6. Reactive sulfhydryl content

Reactive sulfhydryl groups only include those exposed on the surface of the proteins. According to Liu, Zhao, Xie, and Xiong (2011), reactive sulfhydryl groups could form intermolecular disulfide bonds which were crucial for protein aggregation, so the formation of gels could lead to a decrease in reactive sulfhydryl groups. Disulfide bonds played a crucial role in the formation and maintenance of protein gels' functional properties and structure. During the formation process of MP gel, protein molecules unfold, and exposed their internal hydrophobic groups and sulfhydryl groups, which reacted to form disulfide bonds. A three-dimensional network structure with a certain strength was formed as a result of the aggregation of the exposed hydrophobic groups, which helped reduce water loss and enhance the MP gel strength and make the gel structure denser and more ordered. The addition of PP-PSO HIPEs could reduce the content of protein reactive sulfhydryl groups to a certain extent (Table 1). When the addition amount of PP-PSO HIPEs was 10.0 %, the content of reactive sulfhydryl groups reached the lowest
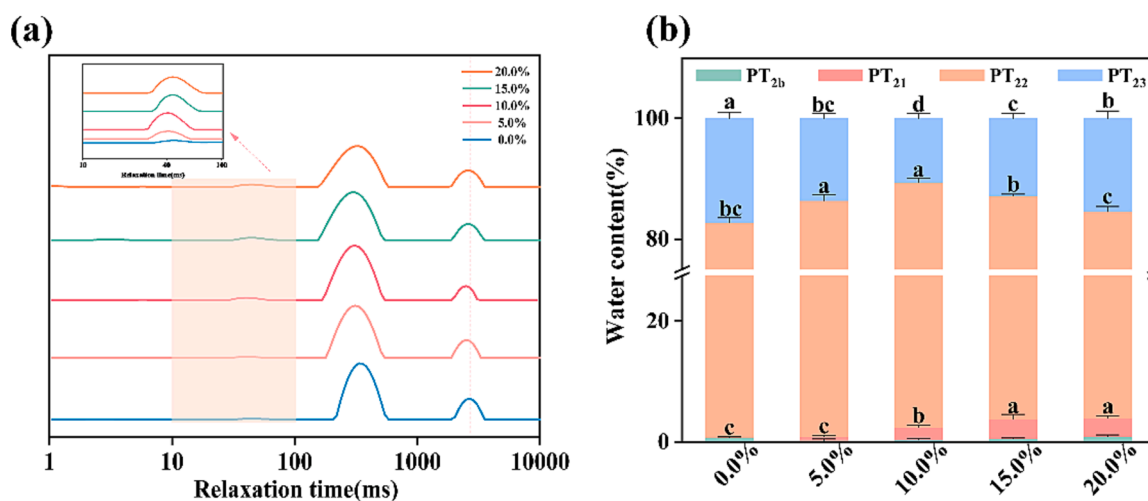

Fig.6. Effect of the addition (0.0% − 20%) of PP-PSO HIPEs on T_2 relaxation time (a) and relaxation percentage (b) of T_{2b}, T_{21}, T_{22} and T_{23} of MP gel. *a-d on the histograms with the same color indicates significant difference ($P < 0.05$).

Table 1

Percentages of protein secondary structures, reactive sulfhydryl contents and surface hydrophobicity contents of MP gels with different content of PP-PSO HIPEs.

PP-PSO HIPEs (%)	α-helix	β-sheet	β-turn	random coil	reactive sulfhydryl	surface hydrophobicity
0.0 %	31.42 ± 0.009[a]	41.68 ± 0.008[b]	7.23 ± 0.010[a]	19.67 ± 0.007[a]	16.50 ± 0.314[a]	30.04 ± 1.302[c]
10.0 %	16.67 ± 0.013[c]	63.15 ± 0.017[a]	6.34 ± 0.010[a]	13.84 ± 0.014[b]	14.82 ± 0.250[b]	47.74 ± 0.659[a]
20.0 %	22.34 ± 0.025[b]	47.06 ± 0.033[b]	8.38 ± 0.042[a]	22.22 ± 0.017[a]	17.11 ± 0.216[a]	32.99 ± 1.561[b]

Different letters represent significant differences (P < 0.05) between the MP gels with different amounts of PP-PSO HIPEs.

value. The main reason might be that the oxidation of sulfhydryl groups to form disulfide bonds, which favors the consolidation of the gel network (Wang et al., 2023b).

4. Conclusion

In conclusion, 4.0 % PP facilitated the formation of a uniform and stable PP-PSO HIPEs, which showed the highest ζ-potential and lowest droplet size. Furthermore, the addition of PP-PSO HIPEs could significantly improve the gel properties of MP gel, and the 10.0 % PP-PSO HIPEs was optimal in terms of the WHC and gel strength. Raman spectra indicated that the addition of PP-PSO HIPEs promoted the transformation of α-helices to β-sheets and increased the hydrophobic interaction in MP gels, thus facilitating the formation of a uniform gel network, which induced the free water partially transformed to immobilized water, finally improved the gel properties of the MP gel. Overall, this work provided a theoretical basis for developing fat-reduced meat products.

CRediT authorship contribution statement

Beibei Li: Writing – original draft, Visualization, Formal analysis, Conceptualization. **Yang Wang:** Writing – review & editing, Visualization, Supervision, Resources, Funding acquisition, Formal analysis, Conceptualization. **Shuyu Wang:** Writing – review & editing, Formal analysis, Conceptualization. **Sengao Chen:** Writing – review & editing. **Chaoyue Yang:** Writing – review & editing. **Linggao Liu:** Writing – review & editing, Conceptualization. **Shenghui Bi:** Writing – review & editing, Formal analysis. **Ying Zhou:** Writing – review & editing, Visualization, Supervision, Resources, Funding acquisition, Formal analysis, Conceptualization. **Qiujin Zhu:** Visualization, Supervision, Methodology, Formal analysis.

Declaration of competing interest

The authors declare that they have no known competing financial interests or personal relationships that could have appeared to influence the work reported in this paper.

Data availability

Data will be made available on request.

Acknowledgements

References

Badar, I. H., Liu, H., Chen, Q., Xia, X., & Kong, B. (2021). Future trends of processed meat products concerning perceived healthiness: A review. *Comprehensive Reviews in Food Science and Food Safety, 20*(5), 4739–4778.

Bibat, M. A. D., Ang, M. J., & Eun, J. B. (2022). Impact of replacing pork backfat with rapeseed oleosomes - Natural pre-emulsified oil - On technological properties of meat model systems. *Meat Science, 186*, 108732.

Buamard, N., & Benjakul, S. (2019). Effect of ethanolic coconut husk extract and pre-emulsification on properties and stability of surimi gel fortified with seabass oil during refrigerated storage. *LWT-Food Science and Technology, 108*, 160–167.

Cai, L., Nian, L., Cao, A., Zhang, Y., & Li, X. (2020). Effect of Carboxymethyl Chitosan Magnetic Nanoparticles Plus Herring Antifreeze Protein on Conformation and Oxidation of Myofibrillar Protein From Red Sea Bream (Pagrosomus major) After Freeze-Thaw Treatment. *Food and Bioprocess Technology, 13*(2), 355–366.

Cando, D., Herranz, B., Javier, B. A., & Moreno, H. M. (2015). Effect of high pressure on reduced sodium chloride surimi gels. *Food Hydrocolloids, 51*, 176–187.

Cen, K., Yu, X., Gao, C., Yang, Y., Tang, X., & Feng, X. (2022). Effects of quinoa protein Pickering emulsion on the properties, structure and intermolecular interactions of myofibrillar protein gel. *Food Chemistry, 394*.

Chen, H., & Han, M. (2011). Raman spectroscopic study of the effects of microbial transglutaminase on heat-induced gelation of pork myofibrillar proteins and its relationship with textural characteristics. *Food Research International, 44*(5), 1514–1520.

Fontes-Candia, C., Martinez-Sanz, M., Gomez-Cortes, P., Calvo, M. V., Verdu, S., Grau, R., & Lopez-Rubio, A. (2023). Polysaccharide-based emulsion gels as fat replacers in Frankfurter sausages: Physicochemical, nutritional and sensorial evaluation. *LWT-Food Science and Technology, 180*.

Gani, A., & Benjakul, S. (2018). Impact of virgin coconut oil nanoemulsion on properties of croaker surimi gel. *Food Hydrocolloids, 82*, 34–44.

WHO (2022). Healthy diet. https://www.who.int/news-room/fact-sheets/detail/healthy-diet.

Hu, M., Xie, F., Zhang, S., Li, Y., & Qi, B. (2020). Homogenization pressure and soybean protein concentration impact the stability of perilla oil nanoemulsions. *Food Hydrocolloids, 101*.

Hu, S., Wu, J., Zhu, B., Du, M., Wu, C., Yu, C., Song, L., & Xu, X. (2021). Low oil emulsion gel stabilized by defatted Antarctic krill (Euphausia superba) protein using high-intensity ultrasound. *Ultrasonics Sonochemistry, 70*.

Kang, Z., Wang, P., Xu, X., Zhu, C., Li, K., & Zhou, G. (2014). Effect of beating processing, as a means of reducing salt content in frankfurters: A physico-chemical and Raman spectroscopic study. *Meat Science, 98*(2), 171–177.

Kornet, R., Yang, J., Venema, P., van der Linden, E., & Sagis, L. M. C. (2022). Optimizing pea protein fractionation to yield protein fractions with a high foaming and emulsifying capacity. *Food Hydrocolloids, 126*.

Lee, H. C., Jang, H. S., Kang, I., & Chin, K. B. (2017). Effect of red bean protein isolate and salt levels on pork myofibrillar protein gels mediated by microbial transglutaminase. *LWT-Food Science and Technology, 76*, 95–100.

Li, X., Liu, W., Xu, B., & Zhang, B. (2022). Simple method for fabrication of high internal phase emulsions solely using novel pea protein isolate nanoparticles: Stability of ionic strength and temperature. *Food Chemistry, 370*.

Lin, J., Meng, H., Yu, S., Wang, Z., Ai, C., Zhang, T., & Guo, X. (2021). Genipin-crosslinked sugar beet pectin-bovine serum albumin nanoparticles as novel pickering stabilizer. *Food Hydrocolloids, 112*.

Liu, R., Zhao, S., Xie, B., & Xiong, S. (2011). Contribution of protein conformation and intermolecular bonds to fish and pork gelation properties. *Food Hydrocolloids, 25*(5), 898–906.

Liu, X., Ji, L., Zhang, T., Xue, Y., & Xue, C. (2019). Effects of pre-emulsification by three food-grade emulsifiers on the properties of emulsified surimi sausage. *Journal of Food Eenineering, 247*, 30–37.

Niknam, R., Ghanbarzadeh, B., Ayaseh, A., & Rezagholi, F. (2018). The effects of Plantago major seed gum on steady and dynamic oscillatory shear rheology of sunflower oil-in-water emulsions. *Journal of Texture Studies, 49*(5), 536–547.

Ran, M., Chen, C., Li, C., He, L., & Zeng, X. (2020). Effects of replacing fat with Perilla seed on the characteristics of meatballs. *Meat Science, 161*.

Ruiz-Capillas, C., Triki, M., Herrero, A. M., Rodriguez-Salas, L., & Jimenez-Colmenero, F. (2012). Konjac gel as pork backfat replacer in dry fermented sausages: Processing and quality characteristics. *Meat Science, 92*(2), 144–150.

Shao, L., Bi, J., Dai, R., & Li, X. (2020). Effects of fat/oil type and ethylcellulose on the gel characteristic of pork batter. *Food Research International, 138*.

Shen, H., Elmore, J. S., Zhao, M., & Sun, W. (2020). Effect of oxidation on the gel properties of porcine myofibrillar proteins and their binding abilities with selected flavour compounds. *Food Chemistry, 329*.

Shi, H., Zhou, T., Wang, X., Zou, Y., Wang, D., & Xu, W. (2021). Effects of the structure and gel properties of myofibrillar protein on chicken breast quality treated with ultrasound-assisted potassium alginate. *Food Chemistry, 358*.

Shi, L., Wang, X., Chang, T., Wang, C., Yang, H., & Cui, M. (2014). Effects of vegetable oils on gel properties of surimi gels. *LWT-Food Science and Technology, 57*(2), 586–593.

Wan, Z., Sun, Y., Ma, L., Guo, J., Wang, J., Yin, S., & Yang, X. (2017). Thermoresponsive structured emulsions based on the fibrillar self-assembly of natural saponin glycyrrhizic acid. *Food & Function, 8*(1), 75–85.

Wang, H., Zhang, J., Liu, X., Wang, J., Li, X., & Li, J. (2024). Effect of sodium starch octenyl succinate-based Pickering emulsion on the physicochemical properties of

hairtail myofibrillar protein gel subjected to multiple freeze-thaw cycles. *Food Science and Human Wellness, 13*(2), 1018–1028.

Wang, H., Zhang, J., Xu, Y., Mi, H., Yi, S., Gao, R., Li, X., & Li, J. (2023). Effects of chickpea protein-stabilized Pickering emulsion on the structure and gelling properties of hairtail fish myosin gel. *Food Chemistry, 417*.

Wang, M., Zhao, Y., Wang, M., Zhang, Z., Huang, M., Wang, K., Shao, J., & Sun, J. (2023). Effects of Tenebrio molitor protein emulsion on the properties, and structure of myofibrillar protein gel. *LWT-Food Science and Technology, 189*, Article 115511.

Wang, Q., Luan, Y., Tang, Z., Li, Z., Gu, C., Liu, R., Ge, Q., Yu, H., & Wu, M. (2023a). Consolidating the gelling performance of myofibrillar protein using a novel OSA-modified-starch-stabilized Pickering emulsion filler: Effect of starches with distinct crystalline types. *Food Research International, 164*, Article 112443.

Wang, Q., Luan, Y., Tang, Z., Li, Z., Gu, C., Liu, R., Ge, Q., Yu, H., & Wu, M. (2023b). Consolidating the gelling performance of myofibrillar protein using a novel OSA-modified-starch-stabilized Pickering emulsion filler: Effect of starches with distinct crystalline types. *Food Research International, 164*.

Wang, S., Liu, L., Bi, S., Zhou, Y., Liu, Y., Wan, J., Zeng, L., Zhu, Q., Pang, J., & Huang, X. (2023). Studies on stabilized mechanism of high internal phase Pickering emulsions from the collaboration of low dose konjac glucomannan and myofibrillar protein. *Food Hydrocolloids, 143*.

Wang, T., Wang, N., Dai, Y., Yu, D., & Cheng, J. (2023). Interfacial adsorption properties, rheological properties and oxidation kinetics of oleogel-in-water emulsion stabilized by hemp seed protein. *Food Hydrocolloids, 137*.

Yang, K., Zhou, Y., Guo, J., Feng, X., Wang, X., Wang, L., Ma, J., & Sun, W. (2020). Low frequency magnetic field plus high pH promote the quality of pork myofibrillar protein gel: A novel study combined with low field NMR and Raman spectroscopy. *Food Chemistry, 326*.

Zhang, R., Cheng, L., Luo, L., Hemar, Y., & Yang, Z. (2021). Formation and characterisation of high-internal-phase emulsions stabilised by high-pressure homogenised quinoa protein isolate. *Colloids and Surfaces A:Physicochemical and Engineering Aspects, 631*.

Zhang, X., Xie, W., Liang, Q., Jiang, X., Zhang, Z., & Shi, W. (2023). High inner phase emulsion of fish oil stabilized with rutin-grass carp (Ctenopharyngodon idella) myofibrillar protein: Application as a fat substitute in surimi gel. *Food Hydrocolloids, 145*.

Zhou, B., Drusch, S., & Hogan, S. A. (2023). Effects of temperature and pH on interfacial viscoelasticity, bulk rheology and tribological properties of whey protein isolate-stabilized high internal phase emulsions. *Food Hydrocolloids, 142*.

Zhu, M., Wang, H., Zong, J., Zhang, J., Zhao, S., & Ma, H. (2024). Evaluating the effects of low-frequency alternating magnetic field thawing on oxidation, denaturation, and gelling properties of porcine myofibrillar proteins. *Food Chemistry, 433*, 137337.

Zhuang, X., Han, M., Kang, Z., Wang, K., Bai, Y., Xu, X., & Zhou, G. (2016). Effects of the sugarcane dietary fiber and pre-emulsified sesame oil on low-fat meat batter physicochemical property, texture, and microstructure. *Meat Science, 113*, 107–115.